Biol. Chem., Vol. 388, pp. 79–89, January 2007 • Copyright © by Walter de Gruyter • Berlin • New York. DOI 10.1515/BC.2007.010

Interaction of the cellular prion protein with raft-like lipid membranes

Kerstin Elfrink, Luitgard Nagel-Steger and Detlev Riesner*

Institut für Physikalische Biologie and Biologisch-Medizinisches Forschungszentrum, Heinrich-Heine-Universität Düsseldorf, Universitätsstr. 1, D-40225 Düsseldorf, Germany

* Corresponding author
e-mail: riesner@biophys.uni-duesseldorf.de

Abstract

Conversion of the cellular isoform of the prion protein (PrP^C) into the disease-associated isoform (PrP^{Sc}) plays a key role in the development of prion diseases. Within its cellular pathway, PrP^C undergoes several posttranslational modifications, i.e., the attachment of two N-linked glycans and a glycosyl phosphatidyl inositol (GPI) anchor, by which it is linked to the plasma membrane on the exterior cell surface. To study the interaction of PrP^C with model membranes, we purified posttranslationally modified PrP^C from transgenic Chinese hamster ovary (CHO) cells. The mono-, di- and oligomeric states of PrP^C free in solution were analyzed by analytical ultracentrifugation. The interaction of PrP^C with model membranes was studied using both lipid vesicles in solution and lipid bilayers bound to a chip surface. The equilibrium and mechanism of PrP^C association with the model membranes were analyzed by surface plasmon resonance. Depending on the degree of saturation of binding sites, the concentration of PrP^C released from the membrane into aqueous solution was estimated at between 10^{-9} and 10^{-7} M. This corresponds to a free energy of the insertion reaction of -48 kJ/mol. Consequences for the conversion of PrP^C to PrP^{Sc} are discussed.

Keywords: Biacore; GPI anchor; prion; PrP^C; surface plasmon resonance.

Introduction

Transmissible spongiform encephalopathies (TSEs), also known as prion diseases, are associated with conversion of the host-encoded prion protein from its cellular isoform PrP^C into an infectious isoform PrP^{Sc} (Prusiner, 1991). The transition between PrP^C and PrP^{Sc} can be regarded as a posttranslational refolding process without any covalent modification (Stahl et al., 1993), but leading to quite different physicochemical properties. PrP^C is mainly of an α-helical secondary structure, soluble in mild detergents and sensitive to protease treatment, whereas PrP^{Sc} has an increased β-sheet content and forms highly insoluble aggregates. On digestion by proteinase K (PK) it is N-terminally truncated at amino acids 89/90 leaving the C-terminal part, PrP 27–30, in a rod like structure with high PK resistance and complete infectivity (McKinley et al., 1983; Caughey et al., 1991; Pan et al., 1993; Safar et al., 1993).

PrP^C is a posttranslationally modified protein carrying two N-glycosylations and a glycosyl phosphatidyl inositol (GPI) anchor. The mature protein is transported to the exterior cell surface, where it is attached to the membrane via the GPI anchor (Stahl et al., 1987). As typical for GPI-anchored proteins, PrP^C is enriched in specific membrane microdomains called rafts (Naslavsky et al., 1997; Gilch et al., 2005). Rafts are liquid-ordered lipid clusters within the membrane with a high content of cholesterol, sphingomyelin and certain lipids with long saturated acyl chains. A specific biochemical property of rafts is their insolubility in Triton X-100 at low temperatures, leading to the synonymous designation as detergent-resistant membranes (DRMs) (Brown and London 1997, 1998; Wang et al., 2000). Several lines of evidence suggest that interaction between PrP^{Sc} and PrP^C, which initiates the conversion process, occurs in lipid rafts: analysis of PrP partitioning in N2a and ScN2a cells by flotation assay showed that both PrP isoforms are co-localized in DRMs (Vey et al., 1996; Naslavsky et al., 1997). Other studies on cultured cells demonstrated that conversion of PrP^C to PrP^{Sc} takes only place when PrP^C is attached to the membrane via the GPI anchor. Membrane attachment in a transmembrane form does not lead to conversion of PrP^C (Kaneko et al., 1997). In addition, a cell-free conversion assay suggested that conversion of PrP^C into a PK-resistant isoform takes place at rafts either after insertion of incoming PrP^{Sc} into the raft domains or by release of PrP^C from the membrane (Baron and Caughey, 2003). Furthermore, small amounts of specific lipids, i.e., galactosylceramide and sphingomyelin, were found as components of natural prions prepared from infected animal brains (Klein et al., 1998).

In the present work we quantitatively analyzed the interaction of PrP^C with raft-like lipid membranes as the first step for future studies on the conversion of PrP on the membrane. We isolated PrP^C carrying both the N-glycosylations and the GPI anchor from CHO cells. The interaction of PrP^C with vesicles of raft-like lipid composition was studied by flotation assay. In addition, systematic studies were carried out on the insertion of PrP^C into surface-bound raft-like membranes by surface plasmon resonance (SPR). We could demonstrate very high affinity and specificity of the interaction between PrP^C and raft-like lipid bilayers and quantitatively describe in thermodynamic and kinetic terms the distribution of PrP^C between the aqueous and lipid phases.

Results

Characterization of the molecular state of purified CHO PrP^C by analytical ultracentrifugation

The interaction of CHO PrP^C with lipid membranes was studied under physiological conditions (pH 6.0, 137 mM NaCl, 37°C). Knowing that CHO PrP^C under these conditions is not stably soluble over a longer period, i.e., several hours, CHO PrP^C stocks were kept under so-called stabilizing conditions (pH 4.0, 4°C), which guarantee solubility over longer times. The samples were diluted to physiological conditions immediately before the interaction studies. Detergents or even mild detergents, which are often used to solubilize membrane proteins, had to be left out completely because they would have an effect on the properties of the model membrane.

A sedimentation velocity experiment involves vacuum pumping, thermal equilibration and the run itself, taking 3–4 h, which clearly exceeds the time needed within the Biacore instrument to apply the sample to the chip surface. Furthermore, the protein concentration necessary for the sedimentation velocity experiment is 50- to 100-fold greater than for SPR measurements. This high protein concentration definitely favors aggregate formation. Therefore, sedimentation velocity experiments were performed under stabilizing conditions at pH 4 instead of pH 6, as used for the membrane binding studies. Figure 1 shows examples of (A) sedimentation profiles and (B) the van Holde-Weischet analysis plot (Demeler and van Holde, 2004). The plot (Figure 1B) shows that approximately 60% of the protein was found in a molecular state with $s_{w,20}$ values ranging from 7.5 to 10 S, 20% with lower $s_{w,20}$ values, i.e., approximately 5 S, and 20% with higher $s_{w,20}$ values but lower than 15 S. The main component corresponds to a molecular state of dimers to tetramers, depending on the shape assumed. The slower portion of the protein corresponds to the monomers and possibly dimers. A small portion of decamers represents the largest aggregates of PrP^C detected. From earlier sedimentation diffusion equilibria, a monomer-dimer equilibrium was reported for PrP^C partially purified from brain (Meyer et al., 2000). In those experiments PrP^C also showed a tendency to aggregate, although the quantitative distribution was different. Since preparation of the sample and performing the SPR experiments takes only a few minutes, whereas oligomerization of PrP takes at least 20 min and multimerization takes several hours (Post et al., 1998), we can safely assume that under the conditions used for membrane interaction studies, the majority of CHO PrP^C is in a monomer-, dimer- and possibly up to tetramer equilibrium.

Furthermore, the secondary structure of CHO PrP^C under the conditions used for SPR experiments was determined by circular dichroism spectroscopy and was found to be mainly α-helical; no shift to an increased β-sheet content could be observed (data not shown).

Reconstitution of CHO PrP^C into raft-like lipid vesicles (RLVs)

Fluorescently labeled RLVs were prepared and CHO PrP^C was added in different ratios and incubated for 30 min.

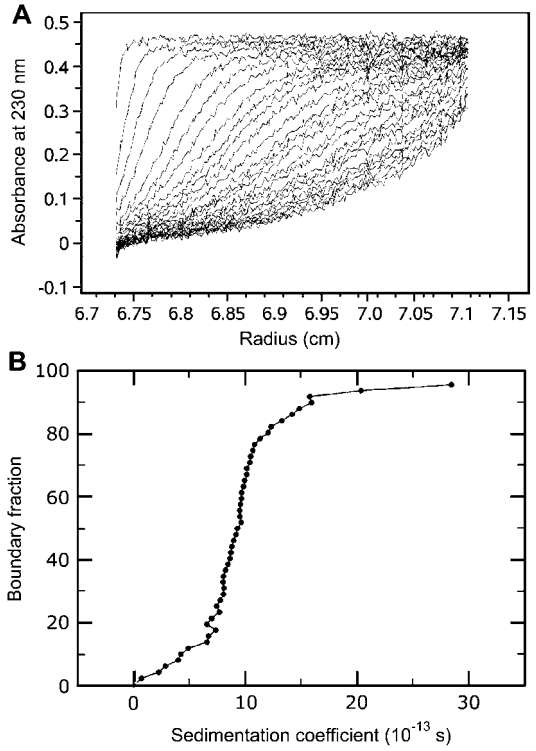

Figure 1 Analysis of the molecular state of CHO PrP^C by analytical ultracentrifugation.
A total volume of 150 µl of CHO PrP^C at a concentration of 60 ng/µl in 10 mM NaAc, pH 4.0 was analyzed by sedimentation velocity experiments at 20 000 rpm and 25°C. Original sedimentation profiles (A) and the van Holde-Weischet analysis plot (B) are shown.

The incubation mixture was fractionated by sucrose density gradient centrifugation. Fractions of these gradients were analyzed for both RLV content by fluorimetric analysis and CHO PrP^C content by SDS-PAGE and Western blotting (Figure 2). RLV accumulated in fractions of approximately 10–15% sucrose (Figure 2A). As a control, CHO PrP^C was incubated and analyzed in the absence of RLVs. Under these conditions, CHO PrP^C was detected only in the pellet fraction. Incubation of CHO PrP^C with RLV at a PrP/lipid molar ratio of 1:20 000 led to an accumulation of CHO PrP^C in the same low-density fractions as for RLVs (Figure 2B). Increasing the amount of RLV to a PrP/lipid molar ratio of 1:80 000 led to complete accumulation of CHO PrP^C in fractions of 10–15% sucrose. This co-localization of CHO PrP^C and RLVs showed that CHO PrP^C binds to RLVs under these conditions and that this binding depends on the stoichiometry. Incubation of RLV with CHO PrP^C transformed by a particular treatment into β-sheet-rich aggregates (Jansen et al., 2001) showed only very low binding activity of CHO PrP^C, leading to the conclusion that the affinity of CHO PrP^C to RLV is mediated by binding of soluble CHO PrP^C in the α-helical conformation. To control the specificity of the interaction with respect to the presence of GPI anchor, we analyzed the binding properties of recPrP(29–231) to RLVs. The finding that no binding of recPrP(29–231) to RLVs could be observed demonstrates that the interaction of CHO PrP^C with RLVs is mediated by the GPI anchor of CHO PrP^C.

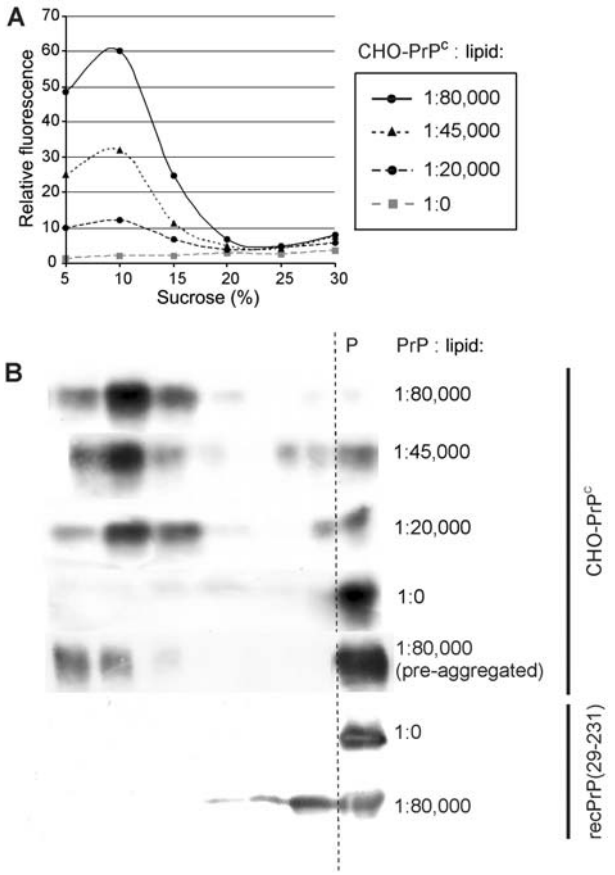

Figure 2 Insertion of CHO PrP^C into raft-like lipid vesicles (RLVs).
CHO PrP^C and recPrP(29–231) were added to fluorescently labeled RLVs at different molar ratios as indicated, and incubated at 37°C for 30 min. Samples were centrifuged for 3 h at 4°C and 160 000 *g* in a sucrose gradient (flotation assay).
(A) RLV quantification by fluorimetric analysis of separated fractions. (B) Detection of PrP by SDS-PAGE and Western blotting (antibody 3F4); P: pellet fraction.

Reconstitution of CHO PrP^C into raft-like lipid bilayers

To analyze the thermodynamics and kinetics of the interaction of CHO PrP^C with surface bound raft-like membranes by SPR, we first prepared a raft-like bilayer on an L1 chip. A stable bilayer was obtained with a response of approximately 8000 response units (RU). Since 1 RU corresponds to 1 pg of bound molecules, it is possible to calculate the number of bound lipid molecules directly from the response observed. Such a calculation yields a result of 6×10^{12} lipid molecules bound/mm^2. This is quite consistent with the number of lipids that would be necessary to cover a surface of 1 mm^2 with a lipid bilayer (4×10^{12} molecules). To ensure that binding of CHO PrP^C to the surface is not due to unspecific binding, probably to uncoated areas of the chip, we first passed CHO PrP^C over a completely uncoated sensor chip (data not shown). The finding that nearly no binding (<30 RU) could be observed in this control demonstrated that all subsequent results are due to interaction of CHO PrP^C with the lipid bilayer.

When the CHO PrP^C solution was injected in a continuous flow over the raft-like bilayer, association of CHO PrP^C was observed in the time range of hundreds of seconds. After switching to a flow of pure buffer, much slower dissociation was measured (Figure 3A). This indicates high affinity of CHO PrP^C for the membrane under physiological conditions. To control the specificity of this interaction, binding of recPrP(29–231), which lacks the GPI anchor and the two N-glycosylations, was analyzed. We observed that binding of recPrP(29–231) indeed (Figure 3A) showed much lower affinity compared to CHO PrP^C.

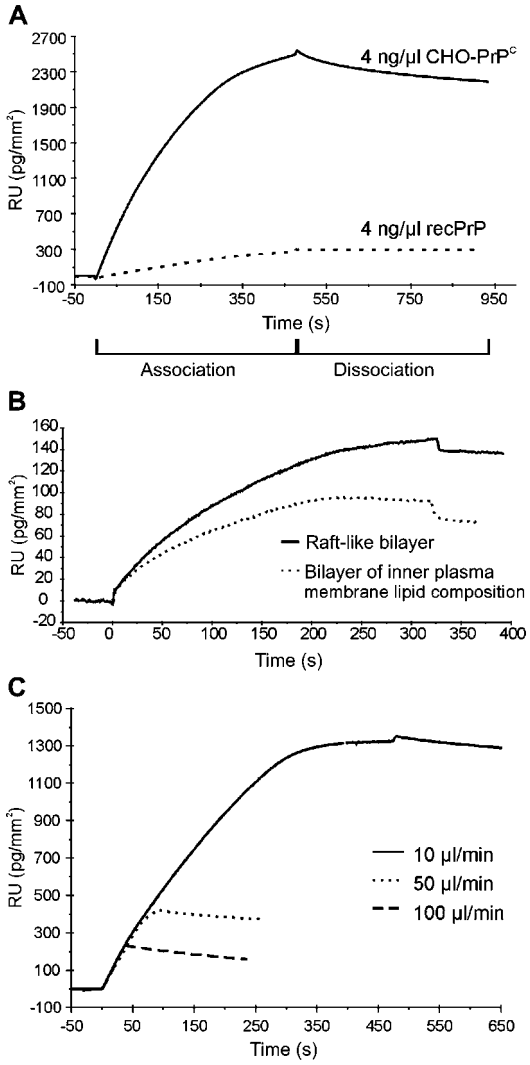

Figure 3 Specific binding of CHO PrP^C to raft-like lipid bilayers as analyzed by SPR.
(A) Comparison of membrane binding of CHO PrP^C and recPrP(29–231). CHO PrP^C and recPrP(29–231) were adjusted to the concentrations indicated in 10 mM sodium citrate, pH 6, 137 mM NaCl (CBS) and a volume of 80 µl was passed immediately over the raft-like bilayer at a flow rate of 10 µl/min. After an association phase of 480 s, CBS was passed over the bilayer at the same flow rate. (B) Influence of the membrane composition on binding of CHO PrP^C. CHO PrP^C was adjusted to a concentration of 0.5 ng/µl and 80 µl were passed over bilayers of different lipid composition as indicated. (C) Influence of the flow rate on binding of CHO PrP^C. CHO PrP^C was adjusted to a concentration of 2 ng/µl in CBS and for each binding curve, an 80-µl sample was passed over the raft-like bilayer at different flow rates, as indicated.

Knowing that GPI-anchored proteins are located *in vivo* in lipid rafts, we compared the affinity of CHO PrP^C to a raft-like bilayer and to a bilayer of a lipid composition of the inner plasma membrane layer. Figure 3B shows that the difference in binding behavior is not very great, but CHO PrP^C has a slightly higher affinity for the bilayer of raft-like lipid composition.

Figure 3C shows no significant difference in association kinetics for CHO PrP^C binding at different flow rates. This indicates that the CHO PrP^C membrane binding studied here is not a transport-controlled process, but is controlled solely by the kinetics of the interaction of CHO PrP^C with the raft-like bilayer.

The nature of the CHO PrP^C membrane interaction was studied in more detail by investigating the influence of different salt conditions on membrane binding of both CHO PrP^C and recPrP(29–231). CHO PrP^C membrane interaction at low ionic strength (0 mM NaCl) did not differ significantly from that observed at higher ionic strength (137 mM NaCl) (Figure 4A). In contrast, ionic strength had a major influence on membrane binding of recPrP(29–231) (Figure 4B). Decreasing ionic strength led to an increase in association of recPrP(29–231), indicating that recPrP(29–231) binds to the bilayer by electrostatic interactions. However, even at low ionic strength, recPrP(29–231) did not reach binding affinities observed for CHO PrP^C (Figure 4C). The very low affinity of recPrP(29–231) for raft-like bilayers at physiological salt concentrations and the very low influence of ionic strength on the affinity of CHO PrP^C to raft-like bilayers led to the conclusion that CHO PrP^C membrane binding is a result of interaction between the GPI anchor of CHO PrP^C and the raft-like bilayer and is mediated by hydrophobic forces.

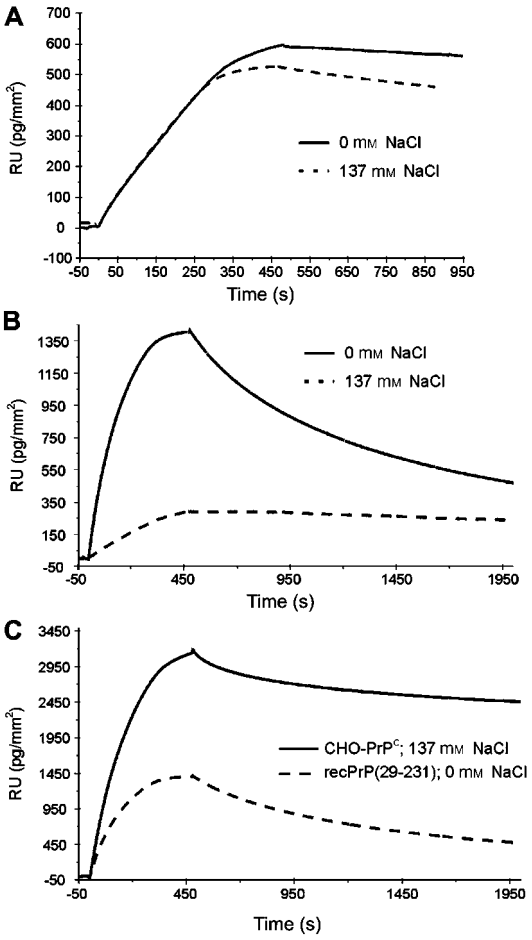

Figure 4 Influence of ionic strength on binding of CHO PrP^C and recPrP(29–231).
For each binding curve, 80 μl were passed over the raft-like bilayer at a flow rate of 10 μl/min. Binding was measured at different salt concentrations. (A) Binding of CHO PrP^C (1 ng/μl) at the NaCl concentrations indicated. (B) Binding of recPrP(29–231) (4 ng/μl) at the NaCl concentrations indicated. (C) Comparison of CHO PrP^C and recPrP(29–231) binding at constant PrP concentration (4 ng/μl) but different NaCl concentrations.

Saturation of CHO PrP^C membrane binding

A single injection of CHO PrP^C apparently reached binding equilibrium. However, we observed that after a short dissociation phase, an additional injection of the same CHO PrP^C concentration led to a further increase in signal, reaching a higher plateau compared to the previous injection (Figure 5A). This means that saturation of CHO PrP^C membrane binding could not be achieved by a single injection. This effect was observed repeatedly during several consecutive injections, but the extent of CHO PrP^C binding during a single injection decreased with additional injections (Figure 5A). To analyze the stepwise saturation in more detail, we extended the association time using a longer continuous flow of sample. As shown in Figure 5B, the extent of CHO PrP^C binding to the membrane during one injection increased considerably. In experiments with shorter continuous flow but at the same flow rate, saturation was apparently achieved much earlier (curve b in Figure 5B). Furthermore, we observed that the effect of stepwise binding of CHO PrP^C as shown in Figure 5A was much less evident at longer injection times (data not shown), i.e., only marginal binding was detected during an additional injection after a sample-flow of 3000 s. The initial binding rate, however, was not affected by the choice of sample flow time. From this we have to conclude that an as yet unidentified effect inhibits CHO PrP^C binding at the end of one injection, whereas the initial binding is unaffected by this effect. More mechanistic details are discussed later.

Taken together, we can conclude that saturation of CHO PrP^C membrane binding can only be achieved either by multiple injections or by a very long continuous flow of sample.

To calculate saturation of CHO PrP^C membrane binding, we superimposed the stepwise binding curves as explained in Figure 5C. The total binding curve was fitted to a one-step second-order binding kinetics and saturation of CHO PrP^C membrane binding was approximately estimated as 4500 RU (pg/mm^2) (Figure 5D). This value corresponds well with that observed at extended sample flow times. With a molecular weight of CHO PrP^C of approximately 35 kDa, saturation corresponds to binding of 7.4×10^{10} CHO PrP^C molecules/mm^2 or one CHO PrP^C molecule/13 nm^2. Knowing that 6×10^{12} lipid molecules are bound per mm^2, this corresponds to a CHO PrP^C/lipid molar ratio of 1:80 relating to a lipid bilayer and 1:40 relating to a lipid monolayer. By estimating the diameter of the membrane-attached PrP^C from molecular

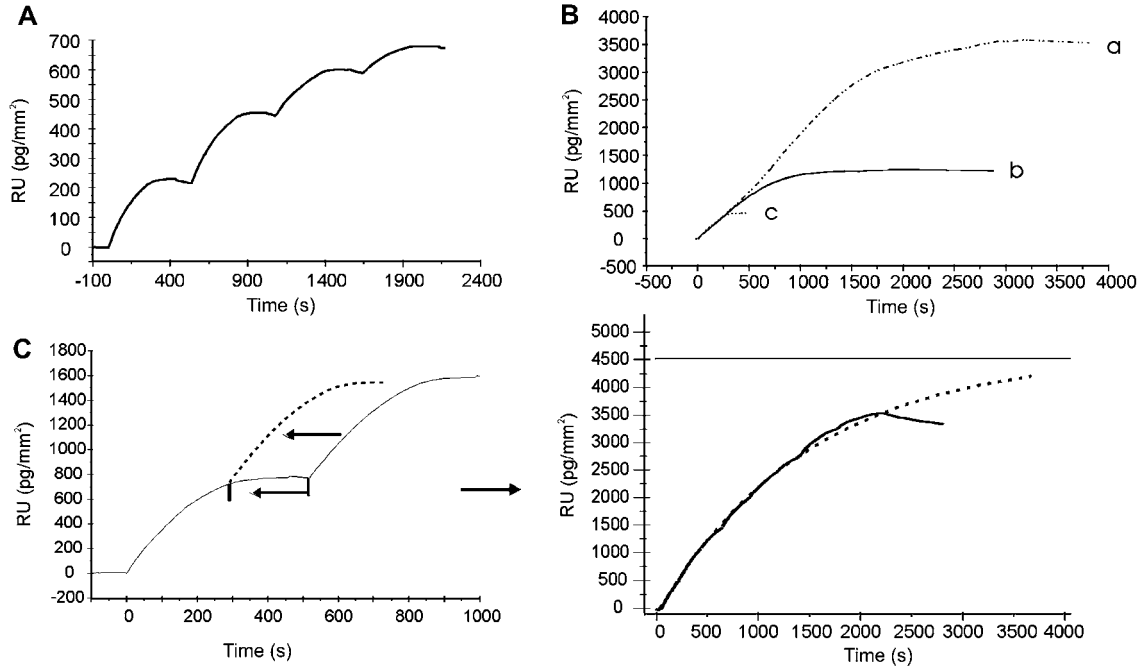

Figure 5 Saturation of CHO PrP^C membrane binding.
(A) Samples of 0.5 ng/μl CHO PrP^C in a volume of 80 μl were injected consecutively at a flow-rate of 10 μl/min. (B) Samples of 1 ng/μl CHO PrP^C but with varying sample volume were injected to analyze the influence of the time range of the continuous sample flow. Samples of 250 μl of CHO PrP^C (curve a) and 160 μl of CHO PrP^C (curve b) were injected at a flow rate of 5 μl/min (Biacore 1000) and 80 μl of CHO PrP^C (curve c) at 10 μl/min (Biacore X). (C) Binding curves of multiple consecutive injections, each of 2 ng/μl CHO PrP^C, were superimposed. From the reconstructed binding curve, saturation of CHO PrP^C membrane binding is estimated to be approximately 4500 pg mm^{-2} (dotted line).

modeling studies (Rudd et al., 2001) and taking into account the known solution structure of the globular domain of Syrian hamster recPrP (Donne et al., 1997; Liu et al., 1999) and the size of the sugar groups, we calculated the area covered by one PrP molecule to be approximately 12 nm^2. Within the limits of error, this number agrees well with the area of 13 nm^2 estimated above, particularly if we take into account that the flexible N-terminus of PrP^C and the larger glycosyl groups of CHO PrP^C compared to PrP^C from hamster brain could not be quantitatively considered. Most probably a continuous monolayer of CHO PrP^C can be assumed.

Evaluation of the kinetic and equilibrium constants

Figure 6A provides examples of binding kinetics for CHO PrP^C at different concentrations. As described in the previous section, the initial binding rate is not affected by the choice of external parameters such as flow rate, injection time and injected volume. Therefore, we determined the kinetic and equilibrium constants by evaluating the initial binding rates. From the initial slope of the binding curves, the association rate $dC_{B,occ}/dt$ ($t \rightarrow 0$) can be determined, where $C_{B,occ}$ is the concentration of occupied binding sites and membrane-bound CHO PrP^C. The relationship between the initial association rate and the association rate constant k_a is defined as:

$$dC_{B,occ}/dt = k_a C_{PrP,free} C_{B,tot} = -(dC_{B,free}/dt) \quad (t \rightarrow 0),$$

where $C_{PrP,free}$ is the concentration of unbound PrP, which is constant during measurement due to the constant flow, $C_{B,tot}$ is the total concentration of membrane binding sites and $C_{B,free}$ is the concentration of free binding sites. As already mentioned, the experimental RU values are equivalent to the concentration of CHO PrP^C bound to the surface ($C_{B,occ}$) in pg mm^{-2}. Initial binding rates, $dC_{B,occ}/dt$ in pg mm^{-2} s^{-1}, were determined at several flow rates and plotted against PrP concentrations (Figure 6B). The slopes of the interpolated straight lines represent $k_a C_{B,tot}$ (Table 1). A value for $C_{B,tot}$ of approximately 7.4×10^{10} binding sites mm^{-2} (=4500 pg mm^{-2}) within the raft-like bilayer was estimated from the saturation curve plotted for multiple PrP injections as described in the previous section. This leads to an association rate constant k_a of 3.9×10^4 M^{-1} s^{-1} (Table 1). The plot shown in Figure 6B for recPrP(29–231) again demonstrates very low binding capacity.

Examination of the dissociation phase reveals that desorption of CHO PrP^C from the membrane takes place by two reaction steps. The initial fast dissociation varied greatly during several experiments. This observation is in agreement with the assumption that CHO PrP^C binds to the membrane in both a specific GPI-anchor-mediated manner and, to a lesser amount, in an unspecific electrostatic manner, with the latter responsible for variations in the initial dissociation phase. Therefore, initial desorption was not included in evaluation of the kinetic dissociation constant determined using the BIAevaluation software (version 4.1). Curve fitting is based on the following equation:

$$RU(t) = RU_{max}\, e^{[-kd(t-t0)]} + \text{offset},$$

where RU_{max} is the signal at the start of the fit and offset is a residual response at infinite time. From 20 independ-

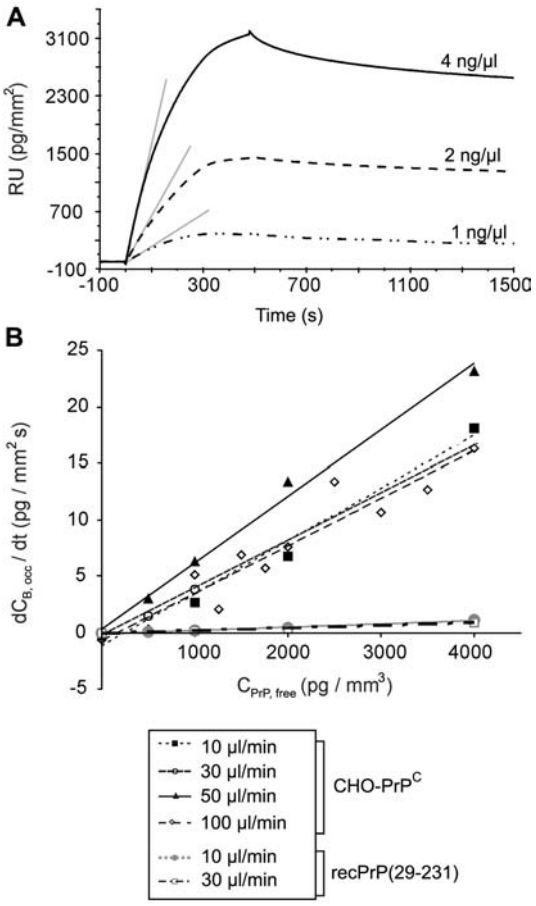

Figure 6 Evaluation of the association rate constants.
(A) Examples of binding kinetics at different CHO PrP^C concentrations are shown. For each binding curve, 80-µl samples were injected at a flow rate of 10 µl/min. Determination of the initial adsorption rates is illustrated (gray straight lines). (B) The initial association rates are plotted against CHO PrP^C concentration to calculate the association rate constants in terms of a second-order reaction (see also Table 1).

ent experiments, k_d values were evaluated and are given in Table 1.

From the knowledge of k_a and k_d, the concentration of free CHO PrP^C in solution but in equilibrium with CHO PrP^C bound to the membrane can be estimated in the following way:

Rate of dissociation:

$$dC_{PrP,diss}/dt = k_d C_{B,occ} = k_d(C_{B,tot}-C_{B,free}).$$

Rate of association:

$$dC_{PrP,ass}/dt = k_a C_{B,free} C_{PrP,free}.$$

Under equilibrium conditions these rates are equal:

$$dC_{PrP,diss}/dt = dC_{PrP,ass}/dt$$

$$k_d\,(C_{B,tot}-C_{B,free}) = k_a C_{B,free} C_{PrP,free}$$

$$C_{PrP,free} = (k_d/k_a)[(C_{B,tot}-C_{B,free})/C_{B,free})]$$

$$= (k_d/k_a)\,[\theta/(1-\theta)],$$

with a degree of saturation $\theta = C_{B,occ}/C_{B,tot} = (C_{B,tot}-C_{B,free})/C_{B,tot}$. With a value for k_d/k_a of 7×10^{-9} M^{-1} according to Table 1, the situation can be described as shown in Table 2. This shows that even at a high degree of saturation, the concentration of free PrP in solution is very low.

From the kinetic constants we can calculate a equilibrium dissociation constant K_d of 7 nM and a Gibbs free energy ΔG° of -48 kJ/mol for the interaction of CHO PrP^C with raft-like lipid membranes. This ΔG° value is in good agreement with results in the literature for binding properties of different membrane proteins or membrane-binding protein domains. Those studies were performed with different equilibrium methods and resulted in values for ΔG° between -27 and -49 kJ/mol (Heymann et al., 1996; Walcher et al., 2001; Zhelev et al., 2001; Goncalves et al., 2005).

Discussion

Analysis of CHO PrP^C-membrane interaction

We investigated the interaction of the cellular isoform of the prion protein with lipid membranes of *in vivo* composition. PrP^C is attached *in vivo* via the GPI anchor to specific microdomains within the plasma membrane, called lipid rafts (Naslavsky et al., 1997). Rafts are lipid clusters enriched in specific lipids such as cholesterol, sphingomyelin and certain lipids with long saturated acyl chains (Brown and London, 1998). Consequently, close to *in vivo* studies of the PrP^C-membrane interaction should be carried out only with PrP that contains the GPI anchor and lipids of raft-like composition. The SPR technique applied in this study allowed quantitative analysis of the PrP^C-membrane interaction.

It was shown by velocity sedimentation experiments and extrapolation to the solution conditions of the SPR studies that the majority of CHO PrP^C is in a monomeric to tetrameric state. This distribution will clearly be shifted further to a monomer-dimer equilibrium if it is taken into account that the SPR experiments were carried out with CHO PrP^C concentrations of 50- to 100-fold lower than the concentrations during sedimentation experiments. In the worst case, the oligomeric forms of CHO PrP^C could lead to a systematic error of a factor of two in underestimating the concentration of free PrP^C and consequently the same factor for the association rate constant and equilibrium binding constant.

Primarily kinetic parameters were determined for the association and dissociation process. From these, equi-

Table 1 Kinetic constants for CHO PrP^C-membrane interaction.

	$k_a\,C_{B,tot}$ (mm s^{-1})	$C_{B,tot}$ (B mm^{-2})	k_a (M^{-1} s^{-1})	k_d (s^{-1})
CHO PrP^C	$4.7\times10^{-3}\pm0.8\times10^{-3}$	7.4×10^{10}	$3.9\times10^{4}\pm0.7\times10^{4}$	$2.6\times10^{-4}\pm1.3\times10^{-4}$
recPrP(29-231)	$0.25\times10^{-3}\pm0.07\times10^{-3}$	n.d.	n.d.	$5.6\times10^{-4}\pm0.5\times10^{-4}$

Results are mean±SD. n.d., not determined.

Table 2 Calculation of the CHO PrP^C-concentration free in solution depending upon binding site saturation.

Degree of saturation θ	$C_{PrP,free}$ (M)
0.1	8×10^{-10}
0.5	7×10^{-9}
0.9	6×10^{-8}

librium constants and saturation parameters could be evaluated. A kinetic analysis of the membrane-binding properties of recPrP(90–231) in different conformations has already been reported in the literature (Critchley et al., 2004). In our understanding, however, the significance of this approach remains unclear, since the mode of interaction of recPrP lacking the GPI anchor cannot resemble the situation *in vivo*. In the present work we investigated binding of recPrP to raft-like lipid bilayers as a control for the specificity of CHO PrP^C membrane interaction. Our observation of very low affinity of recPrP(29–231) for the membrane in comparison to CHO PrP^C indicates that the GPI anchor determines the strength of CHO PrP^C binding to raft-like lipid bilayers. The fact that the affinity of recPrP(29–231) to membranes strongly depends on ionic strength, whereas CHO PrP^C membrane interaction remains nearly unaffected by ionic strength, gives an additional indication of the specificity of CHO PrP^C binding to membranes and of an essential contribution of hydrophobic forces to that interaction. The raft-like composition of the lipids enhances binding of CHO PrP^C to the membrane compared to a lipid composition of the inner plasma membrane; however, it appears to be less critical compared to the influence of the GPI anchor (cf. Figure 3A and B). We do not assume a significant contribution of the glycosyl groups to the affinity of CHO PrP^C to raft-like membranes because large aggregates of CHO PrP^C exhibit very little binding activity (cf. Figure 2B), although the glycosyl groups are not sterically hindered very much.

Surprisingly, we observed that saturation of CHO PrP^C binding to the membrane can only be achieved either by multiple injections or by the choice of very long times (up to 3000 s) of a continuous flow of sample solution. We tried to interpret these effects either on the basis of the biological system or as purely instrumental effects. Considering effects that would be intrinsic in the biological system, we considered whether the liquid flow might exert a flow stress on the membrane surface and consequently that CHO PrP^C may bind initially in a more unspecific way to fewer binding sites. After rearrangement during the switch to a continuous flow of buffer, unspecifically bound CHO PrP^C might be rearranged and inserted into the membrane via the GPI anchor. This mechanism would lead to the availability of a greater number of binding sites at the beginning of the next injection. The finding, however, that apparent saturation was also obtained during short injection times and only reached low RU values (cf. Figure 5B) clearly contradicts such an interpretation.

In discussing instrumental effects, we have to assume a considerable dilution effect at the end of each injection, whereas the first part of the injection is not affected by instrumental effects. To prepare an injection, the sample is first loaded into a sample loop and to prevent dilution of the sample, the Biacore instrument automatically separates the sample from the buffer mobile phase by two air bubbles. These air bubbles are not passed over the bilayer, which means that the switch to a flow of pure buffer from the reservoir occurs before the whole sample is injected. It is well recognized that proteins can adsorb at air-water interfaces (Meinders et al., 2001; de Jongh et al., 2004) and that this adsorption can result in local concentrations at the surface of up to 30 vol.%. In a similar way, dilution of the sample within the last phase of one injection might result from CHO PrP^C adsorption at the interface between the sample and the separating air bubble. This CHO PrP^C-enriched interface region would not be passed over the bilayer. Such effects would lead to different association curves, depending on the choice of external parameters, i.e., the continuous flow time and the injected volume, as we observed in experiments.

The importance of the explanation given should not be overrated, as we tried to explain the stepwise binding as a consequence of the particular experimental method and not as an *in vivo* mechanism. More important is the fact that the kinetic data are not affected by instrumental effects and that saturation of the membrane with CHO PrP^C yields nearly the same value whether extrapolated from stepwise saturation or from long flow-time saturation or from calculating coverage of the membrane by a monolayer of CHO PrP^C.

Two-phase model of PrP conversion

We previously described a model for PrP conversion taking into account the attachment of PrP^C to the plasma membrane on the exterior cell surface (Riesner, 2001). That model, however, was based only on cell biological data for PrP^C localization on the cell surface and on our earlier results showing that the stabilizing effect of low SDS concentrations on the structure of PrP might mimic membrane-like conditions (Post et al., 1998; Leffers et al., 2004). Now that we have quantitatively studied the equilibrium of CHO PrP^C between the states 'free in solution' and 'attached to the membrane', we can quantify the so-called two-phase model of PrP conversion (Figure 7). This model is in contrast with the models that are most often discussed. In the heterodimer model of Cohen et al. (1994), a pre-equilibrium between PrP^C and an activated state PrP* is assumed before a heterodimer PrP^C-PrP^{Sc} is formed. In the model of Jarret and Lansbury (1993), a pre-equilibrium between PrP^C and a monomeric PrP^{Sc}-like state precedes an oligomeric nucleus of PrP^{Sc}. In the two-phase model, the pre-equilibrium is between membrane-bound PrP^C and free PrP^C in solution and the concentration of PrP^C in solution is very low, i.e., in the range of 10^{-9} M. If the membrane is close to saturation, the concentration could be 10^{-8} M or even higher; if the membrane is less occupied, the concentration could be 10^{-10} M or lower (Table 2). The main point of the two-phase model in Figure 7 is that PrP^C in solution is unstable. Either it returns to the membrane-bound state or it can undergo spontaneous transition to amorphous or fibrillar aggregates in the aqueous phase, or it can be bound to an invading prion particle and amplify the PrP^{Sc}

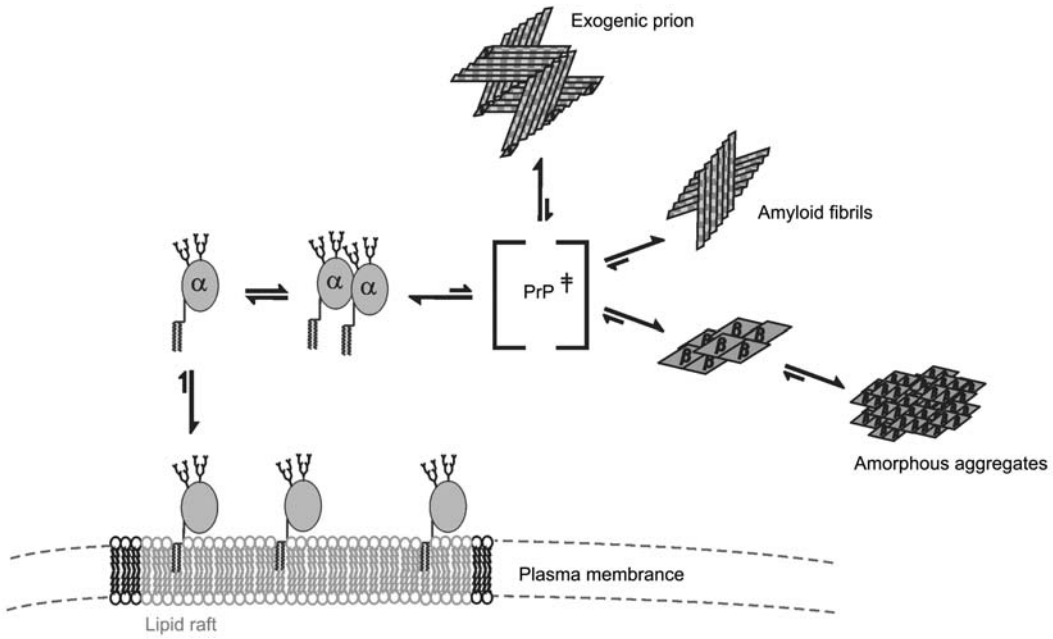

Figure 7 Two-phase model of PrP conversion.
Schematic illustration of different intermediate states involved in PrP conversion. This model takes into account data from the present study and data from previously published studies (Jansen et al., 2001; Leffers et al., 2005).

state. All intermediate states shown here have been proven experimentally (Jansen et al., 2001; Leffers et al., 2005), but we have to admit that these intermediates were stabilized by particular conditions of salt and low SDS concentrations and it cannot be claimed that all intermediates are present under cellular *in vivo* conditions.

It should be mentioned that our studies mimic *in vivo* conditions with two restrictions. First, other PrP^C-binding proteins were not present. Potential PrP^C-binding proteins have been discussed in the literature, such as the 37-kDa laminin receptor precursor, LRP (Rieger et al., 1997), the neural cell adhesion molecule, N-CAM (Schmitt-Ulms et al., 2001) and the tyrosine kinase Fyn (Mouillet-Richard et al., 2000). However, a plasma membrane-localized PrP^C-binding protein would contribute to further stabilization of PrP^C in the membrane-bound state, thereby lowering the concentration of free PrP^C in solution and supporting the situation assumed by the two-phase model. As the second restriction, it must be emphasized that the two-phase-model is the most appropriate way to interpret the solution data and membrane data in a unified model. It is not known, however, whether the conversion of PrP^C to PrP^{Sc} occurs free in solution or in contact with the plasma membrane. However, in the latter case the binding free energy ΔG° of -48 kJ/mol is also of functional importance. That value would act as an energy barrier to liberation of PrP^C from the membrane contacts and incorporation after its structural conversion into the prion particle. It has been shown recently that membrane association of recPrP chemically coupled to a mimetic membrane anchor stabilizes its mainly α-helical structure (Hicks et al., 2006), which might contribute to the ΔG° value.

Results from transgenic mice expressing PrP^C lacking the GPI anchor suggest that membrane contact is not essential for prion amplification, but is essential for pathogenesis (Chesebro et al., 2005). We conclude that in the wild-type case modeled in our studies, spontaneous plaque formation is prevented by keeping PrP^C anchored to the membrane. In transgenic mice, other mechanisms must guarantee concentrations of PrP^C sufficiently high for infection, but sufficiently low for preventing spontaneous disease.

Materials and methods

All chemicals and solutions were obtained from Sigma Aldrich GmbH (Munich, Germany) unless otherwise indicated.

Purification of CHO PrP^C

The Chinese hamster ovary (CHO) cell line overexpressing PrP^C of the Syrian golden Hamster sequence was established by the group of Dr. S.B. Prusiner (Blochberger et al., 1997). PrP^C derived from this cell line (CHO PrP^C) carries the two N-glycosylations and the C-terminal attached GPI anchor. CHO PrP^C was purified using two affinity chromatographic steps: immobilized metal-chelating affinity chromatography (IMAC) using the intrinsic property of PrP^C to bind copper ions and a high-affinity immunopurification using antibody 3F4 covalently coupled to protein G (Elfrink and Riesner, 2004). For each preparation, 4×10^9 CHO cells were solubilized in 10 mM Na-phosphate, pH 7.2 containing 0.5% desoxycholate and 0.5% Nonidet P40 in the presence of protease inhibitors (1 μM pepstatin, 1 μM leupeptin, 2 mM PMSF, 1 mM EDTA). Insoluble constituents were pelleted at 10 000 *g* for 15 min. The supernatant was adjusted to 1 mM imidazole and passed on a copper-loaded IMAC column (chelating Sepharose fast flow; Pharmacia Biotech, Munich, Germany) equilibrated with 20 mM MOPS, pH 7, 150 mM NaCl (MOPBS) at a flow of 2.5 ml/min. To release slightly bound protein, the imidazole concentration was increased stepwise to 10 and 15 mM. PrP^C was eluted using 150 mM imidazole. To prevent aggregation of PrP^C during preparation, each solution contained 0.15% Zwittergent 3–12 (Calbiochem, Darmstadt, Germany). For

immunopurification, antibody 3F4 was cross-linked with protein G-agarose (immunopure protein G IgG plus orientation kit; Pierce, Bonn, Germany). The sample (IMAC-eluate) was loaded onto the column at a flow of 0.5 ml/min. The column was then washed with MOPBS containing 0.15% Zwittergent 3–12 at 2 ml/min and PrP^C was eluted by decreasing the pH to 2.8 (0.1 M HAc, 150 mM NaCl). In contrast to the other solutions used during both chromatography procedures, the elution buffer did not contain Zwittergent 3–12. Since PrP^C is mainly soluble under acidic conditions, it is possible to remove detergent during acidic elution. The pH of the eluted fraction was adjusted to pH 4 and the sample was diluted 1:4 in 1 mM NaAc, pH 4. In the final step the protein was concentrated by centrifugation in Centricon tubes with a cutoff of 10 kDa (Millipore, Schwalbach, Germany).

Purification of recPrP(29–231)

Recombinant prion protein with the Syrian golden Hamster sequence, denoted as recPrP(29–231), was a gift from Dr. S.B. Prusiner and A. Serban (San Francisco, CA, USA). It was expressed and purified as described elsewhere (Mehlhorn et al., 1996). The lyophilized protein was adjusted to a concentration of 5 mg/ml in deionized water and then unfolded by incubation in 6 M guanidinium hydrochloride for 30 min. Refolding of the protein was carried out by fast dilution of the GdnHCl with 25 mM Tris acetate, pH 8.0, 5 mM EDTA to 0.6 M and a protein concentration of 0.5 mg/ml. Subsequently the buffer was exchanged to 1 mM NaOAc, pH 4 by centrifugation in Centricon tubes with a cutoff of 10 kDa (Millipore).

Analytical ultracentrifugation

Sedimentation velocity experiments were performed in a Beckman Optima XL-A analytical ultracentrifuge (Beckman Coulter, Palo Alto, CA, USA) applying 12-mm double-sector aluminum center pieces in an AnTi-60 rotor type and a rotor speed of 20 000 rpm at 25°C. Sedimentation profiles of PrP^C were recorded with a radial step size of 0.001 cm using absorption optics at a wavelength of 230 nm. The PrP^C concentration was 60 ng/μl. Data evaluation according to van Holde-Weischet was performed using the program UltraScan 7.3 (B. Demeler, University of Texas Health Center, San Antonio, TX, USA; http://www.ultrascan.uthscsa.edu/). The vbar value of PrP^C taking into account the two glycosylations and the GPI anchor was calculated using the program SEDNTERP (J. Philo, Alliance Protein Laboratories; http://www.jphilo.mailway.com/) to be 0.6754 cm^3/g at 20°C.

Preparation of large unilamellar vesicles (LUVs)

All lipids used in this study were natural lipids purchased from Avanti Polar Lipids (Otto Nordwald GmbH, Hamburg, Germany). Stock solutions in chloroform were stored at -20°C. LUVs were generated by sonication (Benes et al., 2004). For each experiment, lipids were dried under a stream of nitrogen and evacuated for 15 h. To keep the membranes fluidic, all subsequent procedures were carried out at 37°C. Dried lipids were hydrated to a concentration of 200 μg/ml in 10 mM sodium citrate, pH 6, 137 mM NaCl for 1 h. This leads to the formation of different forms of vesicles: small unilamellar vesicles (SUVs), large unilamellar vesicles (LUVs), giant unilamellar vesicles (GUVs) and multilamellar vesicles (MLVs). After sonication (Labsonic® U, B. Braun Biotech International, Leverkusen, Germany) using a microtip probe (low; 40 W) with a 50% duty cycle for 30 min, mainly LUVs were formed of 100–200 nm in size, as estimated by transmission electron microscopy (data not shown). The solution was then filtered through a 0.45-μm filter (Whatman, Dassel, Germany) to remove any tip-generated debris. Vesicles were used within 1 h to avoid the formation of GUVs and MLVs by relaxation. Raft-like vesicles were of the following lipid composition: dimyristoylphosphatidylcholine (DMPC), sphingomyelin (brain), cerebroside (brain) and cholesterol at a molar ratio of 2:1:1:2 (Schroeder et al., 1994). Vesicles of the inner plasma membrane layer consisted of phosphatidylserine (brain), phosphatidyl-ethanolamine (brain), cerebroside (brain) and cholesterol at a molar ratio of 2:2:1:1.

Reconstitution of CHO PrP^C into large unilamellar raft-like lipid vesicles (RLVs)

Covalently carboxyfluorescein-labeled dioleol-phosphatidyl-ethanolamine (DOPE-CF) was added at a ratio of 0.07 μg per mg of the raft-like lipid mixture prior to LUVs prepared as described above. CHO PrP^C was added to DOPE-CF-labeled LUVs and incubated for 30 min. LUVs were separated by centrifugation in a sucrose density gradient (flotation assay). Samples were adjusted to 30% sucrose and stepwise overlaid with 200 μl of 20%, 15%, 10% and 5% sucrose. After centrifugation for 3 h at 4°C and 160 000 *g* (TLS-55; Beckmann Optima™ TL; Palo Alto, CA, USA) 200-μl fractions were collected and the pellet was resuspended in SDS-PAGE loading buffer.

Binding kinetics

Kinetic analyses of CHO PrP^C membrane interaction were performed mainly on a Biacore X or a Biacore 1000 system, as indicated (Biacore International S.A., Freiburg, Germany). The Biacore method is based on the physical phenomenon of surface plasmon resonance (SPR) and detects binding of molecules to a surface by measuring changes in the resonance angle (Otto, 1968). The resonance angle depends on the refractive index above the surface up to a maximum distance from the surface of 300 nm. This method allows time-dependent measurements of biomolecular adsorption to a surface. The resulting sensogram is a plot of the SPR signal in relative units (RU) against time. A relative unit is equivalent to 1 pg of molecules bound to the surface of the flow cell, which has an area of 1 mm^2. Therefore, RU can be described as pg/mm^2. The chip used for all binding studies was the L1 sensor chip (Biacore International S.A.). This chip, typically used for studying protein membrane interaction (MacLeod et al., 2003; Kölzer et al., 2004), is coated with a dextran layer spiked with certain lipophilic components and allows fusion of liposomes by forming a flexible lipid bilayer (Erb et al., 2000; Saenko et al., 2001). The chip was first cleaned by injection of 80 μl of 20 mM CHAPS. Then LUVs were passed over the surface. For stabilization, 80 μl of 50 mM NaOH was applied. Finally, 1 mg/ml BSA was injected to block non-specific binding to the surface. Samples of CHO PrP^C were diluted in 10 mM sodium citrate, pH 6 and 137 mM NaCl to different concentrations and for each experiment 80 μl was immediately injected at different flow rates, as indicated.

Acknowledgments

We thank Prof. Stanley B. Prusiner and A. Serban (San Francisco, USA) for the kind gift of the CHO cell line, Dr. Jens Schell for establishing the CHO cell line in our laboratory and Prof. D. Willbold for access to the Biacore X instrument. We gratefully acknowledge B. Demeler for support with the UltraScan software and help in evaluating sedimentation analysis data. This work was supported by Bundesministerium für Bildung und Forschung (grants PT31/0312721 and 13N7515/6), Ministerium für Umwelt und Naturschutz (grant VI-1-0540.01) and NoE NeuroPrion.

References

Baron, G.S. and Caughey, B. (2003). Effect of glycosylphosphatidylinositol anchor-dependent and -independent prion protein association with model raft membranes on conversion to the protease-resistant isoform. J. Biol. Chem. *278*, 14883–14892.

Benes, M., Billy, D., Benda, A., Speijer, H., Hof, M., and Hermens, W.T. (2004). Surface-dependent transitions during self-assembly of phospholipid membranes on mica, silica, and glass. Langmuir *20*, 10129–10137.

Blochberger, T.C., Cooper, C., Peretz, D., Tatzelt, J., Griffith, O.H., Baldwin, M.A., and Prusiner, S.B. (1997). Prion protein expression in Chinese hamster ovary cells using a glutamine synthetase selection and amplification system. Protein Eng. *10*, 1465–1473.

Brown, D.A. and London, E. (1997). Structure of detergent-resistant membrane domains: does phase separation occur in biological membranes? Biochem. Biophys. Res. Commun. *240*, 1–7.

Brown, D.A. and London, E. (1998). Structure and origin of ordered lipid domains in biological membranes. J. Membr. Biol. *164*, 103–114.

Caughey, B.W., Dong, A., Bhat, K.S., Ernst, D., Hayes, S.F., and Caughey, W.S. (1991). Secondary structure analysis of the scrapie-associated protein PrP 27–30 in water by infrared spectroscopy. Biochemistry *30*, 7672–7680.

Chesebro, B., Trifilo, M., Race, R., Meade-White, K., Teng, C., LaCasse, R., Raymond, L., Favara, C., Baron, G., Priola, S., et al. (2005). Anchorless prion protein results in infectious amyloid disease without clinical scrapie. Science *308*, 1435–1439.

Cohen, F.E., Pan, K.M., Huang, Z., Baldwin, M., Fletterick, R.J., and Prusiner, S.B. (1994). Structural clues to prion replication. Science *264*, 530–531.

Critchley, P., Kazlauskaite, J., Eason, R., and Pinheiro, T.J.T. (2004). Binding of prion proteins to lipid membranes. Biochem. Biophys. Res. Commun. *313*, 559–567.

de Jongh, H.H.J., Kosters, H.A., Kudryashova, E., Meinders, M.B.J., Trofimova, D., and Wierenga, P.A. (2004). Protein adsorption at air-water interfaces: a combination of details. Biopolymers *74*, 131–135.

Demeler, B. and van Holde, K.E. (2004). Sedimentation velocity analysis of highly heterogeneous systems. Anal. Biochem. *335*, 279–288.

Donne, D.G., Viles, J.H., Groth, D., Mehlhorn, I., James, T.L., Cohen, F.E., Prusiner, S.B., Wright P.E., and Dyson, H.J. (1997). Structure of the recombinant full-length hamster prion protein PrP(29–231): the N terminus is highly flexible. Proc. Natl. Acad. Sci. USA *94*, 13452–13457.

Elfrink, K. and Riesner, D. (2004). Purification of PrP^{C}. In: Techniques in Prion Research, S. Lehmann and J. Grassi, eds. (Basel, Switzerland: Birkhäuser Verlag), pp. 4–15.

Erb, E.M., Chen, X., Allen, S., Robert, C.J., Tendler, S.J., Davies, M.C., and Forsen, S. (2000). Characterization of the surfaces generated by liposome binding to the modified dextran matrix of a surface plasmon resonance sensor chip. Anal. Biochem. *280*, 29–35.

Gilch, S., Kehler, C., and Schätzl, H.M. (2005). The prion protein requires cholesterol for cell surface localization. Mol. Cell. Neurosci. *30*, 346–353.

Goncalves, E., Kitas, E., and Seelig, J. (2005). Binding of oligoarginine to membrane lipids and heparan sulfate: structural and thermodynamic characterization of a cell-penetrating peptide. Biochemistry *44*, 2692–2702.

Heymann, J.B., Zakharov, S.D., Zang, Y.L., and Cramer, W.A. (1996). Characterization of electrostatic and nonelectrostatic components of protein-membrane binding interactions. Biochemistry *35*, 2717–2725.

Hicks, M.R., Gill, A.C., Bath, I.K., Rullay, A.K., Sylvester, I.D., Crout, D.H., and Pinheiro, T.J.T. (2006). Synthesis and structural characterization of a mimetic membrane-anchored prion protein. FEBS J. *273*, 1285–1299.

Jansen, K., Schäfer, O., Birkmann, E., Post, K., Serban, A., Prusiner, S.B., and Riesner, D. (2001). Structural intermediates in the putative pathway from the cellular prion protein to the pathogenic form. Biol. Chem. *382*, 683–691.

Jarret, J.T. and Lansbury, P.T. (1993). Seeding 'one-dimensional crystallisation' of amyloid: a pathogenic mechanism in Alzheimer's disease and scrapie? Cell *73*, 1055–1058.

Kaneko, K., Vey, M., Scott, M., Pilkuhn, S., Cohen, F.E., and Prusiner, S.B. (1997). COOH-terminal sequence of the cellular prion protein directs subcellular trafficking and controls conversion into the scrapie isoform. Proc. Natl. Acad. Sci. USA *94*, 2333–2338.

Klein, T.R., Kirsch, D., Kaufmann, R., and Riesner, D. (1998). Prion rods contain small amounts of two host sphingolipids as revealed by thin-layer chromatography and mass spectrometry. Biol. Chem. *379*, 655–666.

Kölzer, M., Werth, N., and Sandhoff, K. (2004). Interactions of acid sphingomyelinase and lipid bilayers in the presence of the tricyclic antidepressant desipramine. FEBS Lett. *559*, 96–98.

Leffers, K.W., Schell, J., Jansen, K., Lucassen, R., Kaimann, T., Nagel-Steger, L., Tatzelt, J., and Riesner, D. (2004). The structural transition of the prion protein into its pathogenic conformation is induced by unmasking hydrophobic sites. J. Mol. Biol. *26*, 839–853.

Leffers, K.W., Wille, H., Stoehr, J., Junger, E., Prusiner S.B., and Riesner, D. (2005). Assembly of natural and recombinant prion protein into fibrils. Biol. Chem. *386*, 569–580.

Liu, H., Farr-Jones, S., Ulyanov, N.B., Llinas, M., Marqusee, S., Groth, D., Cohen, F.E., Prusiner, S.B., and James, T.L. (1999). Solution structure of Syrian hamster prion protein rPrP-(90–231). Biochemistry *38*, 5362–5377.

MacLeod, T.J., Kwon, M., Filipenko, N.R., and Waisman, D.M. (2003). Phospholipid-associated annexin A2-S100A10 heterotetramer and its subunit. J. Biol. Chem. *278*, 25577–25584.

McKinley, M.P., Bolton, D.C., and Prusiner, S.B. (1983). A protease-resistant protein is a structural component of the scrapie prion. Cell *35*, 57–62.

Mehlhorn, I., Groth, D., Stockel, J., Moffat, B., Reilly, D., Yansura, D., Willett, W.S., Baldwin, M., Fletterick, R., Cohen, F.E., et al. (1996). High-level expression and characterization of a purified 142-residue polypeptide of the prion protein. Biochemistry *30*, 5528–5537.

Meinders, M.B.J., van den Bosch, G.G.M., and de Jongh, H.H.J. (2001). Adsorption properties of proteins at and near the air/water interface from IRRAS spectra of protein solutions. Eur. Biophys. J. *30*, 256–267.

Meyer, K.M., Lustig, A., Oesch, B., Fatzer, R., Zurbriggen, A., and Vandevelde, M. (2000). A monomer-dimer equilibrium of a cellular prion protein (PrPC) not observed with recombinant PrP. J. Biol. Chem. *275*, 38081–38087.

Mouillet-Richard, S., Ermonval, M., Chebassier, C., Laplanche, J.L., Lehmann, S., Launay, J.M., and Kellermann, O. (2000). Signal transduction through prion protein. Science *289*, 1925–1928.

Naslavsky, N., Stein, R., Yanai, A., Friedlander, G., and Taraboulos, A. (1997). Characterization of detergent-insoluble complexes containing the cellular prion protein and its scrapie isoform. J. Biol. Chem. *272*, 6324–6331.

Otto, A. (1968). A new method for exciting non-radioactive surface plasma oscillations. Phys. Stat. Sol. *26*, 99–101.

Pan, K.M., Baldwin, M.A., Nguyen, J., Gasset, M., Serban, A., Groth, D., Mehlhorn, I., Huang, Z., Fletterick, R.J., Cohen, F.E., and Prusiner, S.B. (1993). Conversion of α-helices into β-sheet features in the formation of the scrapie prion proteins. Proc. Natl. Acad. Sci. USA *90*, 10962–10966.

Post, K., Pitschke, M., Schaefer, O., Wille, H., Appel, T.R., Kirsch, D., Mehlhorn, I., Serban, H., Prusiner, S.B., and Riesner, D. (1998). Rapid acquisition of β-sheet structure in the prion protein prior to multimer formation. Biol. Chem. *379*, 1307–1317.

Prusiner, S.B. (1991). Molecular biology of prion diseases. Science *252*, 1515–1522.

Rieger, R., Edenhofer, F., Lasmezas, C.I., and Weiss, S. (1997). The human 37-kDa laminin receptor precursor interacts with the prion protein in eukaryotic cells. Nat. Med. *3*, 1383–1388.

Riesner, D. (2001). Die Scrapie-Isoform des Prion-Proteins PrP^{Sc} im Vergleich zur zellulären Isoform PrP^C. In: Prionen und Prionkrankheiten, B. Hörnlimann, D. Riesner and H. Kretzschmar, eds. (Berlin, Germany: Walter de Gruyter), pp. 81–91.

Rudd, P.M., Wormald, M.R., Wing, D.R., Prusiner, S.B., and Dwek, R.A. (2001). Structure, dynamics and roles for the sugars. Biochemistry *40*, 3759–3766.

Saenko, E. Sarafanov, A., Ananyeva, N., Behre; E., Shima, M., Schwinn, H., and Josic, D. (2001). Comparison of the properties of phospholipid surfaces formed on HPA and L1 biosensor chips for the binding of the coagulation factor VIII. J. Chromatogr. A *921*, 49–56.

Safar, J., Roller, P.P., Gajdusek, D.C., and Gibbs, C.J. Jr. (1993). Thermal stability and conformational transitions of scrapie amyloid (prion) protein correlate with infectivity. J. Biol. Chem. *268*, 20276–20284.

Schmitt-Ulms, G., Legname, G., Baldwin, M.A., Ball, H.L., Bradon, N., Bosque, P.J., Crossin, K.L., Edelmann, G.M., DeArmond, S.J., Cohen, F.E., and Prusiner, S.B. (2001). Binding of neural cell adhesion molecules (N-CAMs) to the cellular prion protein. J. Mol. Biol. *314*, 1209–1225.

Schroeder, R., London, E., and Brown, D. (1994). Interactions between saturated acyl chains confer detergent resistance on lipids and glycosylphosphatidylinositol (GPI)-anchored proteins: GPI-anchored proteins in liposomes and cells show similar behavior. Proc. Natl. Acad. Sci. USA *91*, 12130–12134.

Stahl, N., Borchelt, D.R., Hsiao, K., and Prusiner, S.B. (1987). Scrapie prion protein contains a phosphatidylinositol glycolipid. Cell *51*, 229–240.

Stahl, N., Baldwin, M.A., Teplow, D.B., Hood, L., Gibson, B.W., Burlingame, A.L., and Prusiner, S.B. (1993). Structural studies of the scrapie prion protein using mass spectrometry and amino acid sequencing. Biochemistry *32*, 1991–2002.

Vey, M., Pilkuhn, S., Wille, H., Nixon, R., DeArmond, S.J., Smart, E.J., Anderson, R.G., Taraboulos, A., and Prusiner, S.B. (1996). Subcellular colocalization of the cellular and scrapie prion proteins in caveolae-like membranous domains. Proc. Natl. Acad. Sci. USA *93*, 14945–14949.

Walcher, S., Altschuh, J., and Sandermann, H. Jr. (2001). The lipid/protein interface as xenobiotic target site: kinetic analysis of the nicotinic acetylcholine receptor. J. Biol. Chem. *276*, 42191–42195.

Wang, T.Y., Leventis, R., and Silvius, J.R. (2000). Fluorescence-based evaluation of the partitioning of lipids and lipidated peptides into liquid-ordered lipid microdomains: a model for molecular partitioning into lipid rafts. Biophys. J. *79*, 919–933.

Zhelev, D.V., Stoicheva, N., Scherrer, P., and Needham, D. (2001). Interaction of synthetic HA2 influenza fusion peptide analog with model membranes. Biophys. J. *81*, 285–304.

Received May 9, 2006; accepted September 19, 2006